Estimation of Turbine Rotor Tendency to Brittle Fracture

Yu. N. Rabotnov, G. S. Vasilchenko, P. F. Koshelev,
G. N. Merinov and Yu. P. Rybovalov
(Moscow)

In the next years the development of the power engineering will involve the increase of the turbine sizes, use of the welded rotor structures and stronger materials. All this deems it necessary to solve the problem of estimating the turbine rotor tendency to brittle fracture in the presence of the defects.

The experiments have involved the analysis of the full--scale forgings made of steels 18FDOV, 34HMA, 24H2NMFA and full-section welded joints obtained by manual welding using the CL-30 electrode and by automatic welding using the IOHM and O8HN2M wire. There have been considered the experimental data on the qualitative and quantitative methods of estimation of the tendency of the materials to brittle fracture, the results of the experiments being processed in accordance with concepts of the linear fracture mechanics. Particular attention has been paid to establishing the relationship between 50 % shear texture transition temperature (50 % FATT) and stress intensity factor K_{Ic}. Several rotors have been checked for brittle fracture tendency with the use procedure which provides for determination of the structure safety factors in the presence of the defects, with due regard to the properties of the material.

1. Impact test results

Standard specimens with the Charpy-V or Mesnager notches and specimens with the fatigue cracks were

tested under the impact bending conditions. The notches were made in the base and welded metal as well as in the heat affected zone. The obtained data were used to plot the variation of the impact toughness and percentage of the shear texture in the fracture versus temperature. By way of example, Fig. 1a illustrates the above relationships for the welded joint (steel 34HMA) obtained by manual welding with the use of the CL-30 electrode. As would be expected, the curves were arranged in succession depending on the sharpness of the notch. Similar results were obtained for the base metal and for the heat affected zone. Transition temperatures $V_{2.8}TT$ as determined for a particular energy level, e.g. 2.8 kgm (a_n=3.5 kgm/cm^2) for the tested specimens (Fig. 1a) differ in 50 - 85 ^{o}C which proves that the transition temperature greatly depends on the sharpness of the notch. When the transition temperatures are determined by 50 % shear texture, the range of the temperature variation is markedly reduced and does not exceed 22 ^{o}C (see Fig. 1b). Low dependance of the transition temperature determined by 50 % shear texture on the sharpness of the notch is well comparatible with the data presented in the literature (1).

50 % FATT of the Charpy-V notch specimens equals -6 ^{o}C for the metal of the heat affected zone, +7 ^{o}C for the deposited metal and +63 ^{o}C for the base metal which proves that the metal of the heat affected zone and the deposited metal show a lower tendency to brittle fracture as compared to the base metal.

It is worth while mentioning that 50 % FATT of the Charpy-V notch spesimens lies in the middle of the transition temperature range for the tested specimens. Therefore, it is recommended that 50 % FATT be determined on the Charpy-V notch specimens. When determining 50 % FATT

on the Menager's specimens, the obtained values should be decreased approximately by 8 - 10 ^{o}C.

2. Spin burst testing results.

There were tested solid and welded flat disks, dia. 600 mm, 75 mm thick, with two notches having a root curvature radius of 0,12 mm and made from the central hole, dia. 100 mm. The fracture of the disks was accomplished in a spinning set (2) at temperatures of +20 ^{o}C and -30 ^{o}C. Critical stress intensity factors K_{Ic} and critical strain energy release rate G_{Ic} were calculated by the formulas eshibited in (3). The validity of the values of K_{Ic} were checked according to the following equation (4):

$$c \text{ and } B \geqslant 2.5 \, (K_{Ic}/\sigma_{0.2})^2$$

where c - the depth of the notch, i.e. the distance from the centre of the disk to the notch root; B - the thickness of the disk at the notch region.

The obtained data are shown in Fig. 2 versus excessive temperature $T_e = T_o$ - 50 % FATT, where T_o is the operating temperature. The valid values of K_{Ic} are shown below the solid line. As it may be seen from Fig. 2, the spin tests of the notched disks may be employed for determination of valid values of K_{Ic}. Besides, these data testify to high quality of the welded joint made in accordance with the approved technological procedures, since the values of K_{Ic} for the welded disks do not exceed the limits of the K_{Ic} values for the solid disks.

3. Results testing of the specimens, types WOL and CT.

The use of complex equipment and large dimensions of the disks do not make it possible to conduct spin tests within a wide scope. To avoid performance of the spin

tests, E.T. Wessel (4) suggests to use the specimens, type WOL, which feature low metal consumption and require a few test equipment, ensuring a tensile force of up to 100 tons.

Test specimens, types WOL-2X and WOL-4X were fabricated from 24Hn2MFA and 18FDOV steelsforgings and test specimens, types CT-2T and CT-3T, were made from steel 18FDOV. Fatigue cracks in the root of the chevron notches were obtainted on the hydraulic machine with the pulsator, at a stepped reduction of the maximum force of the cycle. Test specimens made of steel 24HN2MFA with the fatigue cracks were fractured at temperatures of 20 °C; -30 and -60 °C, whereas test specimens made of steel 18FDOV were fractured at temperatures of 20 to -155 °C.

A displacement gauge was installed in the root of the notch and the relationship between the load and notch opening displacement was recorded in the course of the tests. This relationship was necessary to determine the load used during calculation of K_{Ic} in accordance with the procedure echibited in (4). The test results pertaining to determination of K_{Ic} and material yield stress are shown in Fig. 3. As it is seen in this Fig. 3, for steel 24HN2MFA the valid values of K_{Ic} obtained on the disks and WOL specimens are practically identical at temperatures of 20 and -30 °C. The disks were not tested at a temperature of -60 °C, however the values of K_{Ic} obtained at this temperature resulting from extrapolation also coincide with the valid values of K_{Ic} for the specimens. It is of interest that the WOL-2X specimens made of steel 24HN2MFA with the crack 0.7W long, being tested at 20 °C, have made it possible to determine the average value of K_{Ic} and the range of the K_{Ic} values which coincide with the valid measured on specimens WOL-4X and disks. Thus,

the above data suggest that it is quite possible to resort to testing specimens, type WOL, instead of performing disk spinning tests. This conclusion is in full conformity with the concepts of publication (4).

The data pertaining to steel 18FDOV which are shown in Fig. 3 testify to high resistivity of this steel to development of cracks in that the valid values of K_{Ic} for the WOL-4X and CT-2T specimens were obtained only at a temperature of -120 °C, while for the WOL-2X specimen it was necessary to reduce the test temperature down to -155 °C, i.e. the valid values of K_{Ic} were obtained at sufficiently large dimensions of the specimens and at a substantial decrease the test temperature.

Since the values of the resistance to development of cracks as computed by reference to the force which characterizes the initial non-stability moment were mostly different from the valid values, there was made an attempt at determining K_{Ic} for the test specimens by reference to the δ_t crack opening displacement diagrams. As it is shown in (5), crack opening may be determined by the formula:

$$\delta_t = \frac{V_g}{1 + \frac{a + z}{r\,(W - a)}}$$

where V_g is clip gauge displacement;

z is the distance above the specimen surface at which the measurment is made

a is total crack length

W is the specimen width

r is the rotational factor relating V_g to δ_t

Fig. 4 shows variation of the rotational factor with

clip gauge reading for CKS tension tests (5).

Shown in Fig. 5 are the values of K_{Ic} versus the test temperature. The K_{Ic} values were determined by reference to the measured forces and were calculated by the formula

$$K_{Ic} = \sqrt{\delta_t \cdot \sigma_{0.2} \cdot E}$$

were E is the modulus of elasticity and $\sigma_{0.2}$ is the metal yield stress. The crack opening displacement was determined both at a variable rotational factor and at a constant rotational factor equal to 1/3. From Fig. 5 it follows that in the region of valid values, the K_{Ic} values determined by reference to the measured forces and by reference to δ_t values calculated with regard to variation of the radius of rotational are practically identical. The K_{Ic} values determined without taking into account the radius of rotational are considerably greater than the K_{Ic} values determined with due regard to this factor.

4. Generalized diagram of fracture toughness.

The results of the present investigations and data presented in (6, 9) have made it possible to plot a generalized diagram of fracture toughness of perlite steels with the yield stresses of 40 to 120 kg/mm^2 and 50 % FATT in the range from -60 to +100 ^{o}C (see Fig. 6). This diagram shows the variation of the stress intensity factor K_{Ic} versus excessive temperature T_e. The diagram may be referred to within the working temperature range of -150 to + 100 ^{o}C. Particular interest is presented by curves 1 and 2 plotted by reference to the results respectively of testing of specimens with the Menager den Charpy-V notches. These curves limit the lower level of the wide band of spreaded values. In the range of the valid values, i.e. up to K_{Ic} = 450 kg/mm$^{3/2}$, curve

I may be expressed analitically accurate to 3 % with the use of the following formula:

$$K_{Ic\ min} = \frac{20400}{86 - T_e} \ (kg/mm^{3/2})$$

These curves may be used for determination of the guaranted minimum value of K_{Ic} by reference to the operating temperature and 50 % FATT obtained during test of the specimens on the impact bend. The K_{Ic} value determined by this manner may be employed for determination of the safety factors of the rotors which are being designed. This safety factor determination will be quite reliable and may be further specified after finding the valid value of the fracture toughness of a specific material.

The generalized diagram shown in Fig. 7 makes it possible to compare the curves with the results of impact tests of the specimens having notches of the Charpy-V, Mesnager and a fatigue crack. If the middle of the transition temperature in the generalized diagram is determined by reference to K_{Ic} = 425 Kg/mm$^{3/2}$ corresponds to a temperature of T_e = -15 ^{o}C, then the average values of the impact toughness for the Mesnager notch specimens correspond to a_n = 12 kgm/cm^2, for the Charpy-V notch specimens to a_n = 7 kgm/cm^2, and for the specimens with fatigue crack to a_n=3 kgm/cm^2. This makes it possible to estimate the critical resistivity of the material to crack development by reference to the indicated values of the impact toughness. It is worth mentioning that the above considerations are rather approximalte and require further statistical processing. From Fig. 7 it follows that the impact toughness data obtained on the specimens with the Charpy-V notches more adequately correspond to the middle of the transition temperature estimated

by reference to the generalized diagram than the data obtained on the other specimens, which shows the expediency of using these specimens for determination of the transition temperatures.

5. Testing small-size prismatic specimens for static load bending.

With a view to checking the possibility of using small-size specimens instead of large specimens employed for determination of the fracture toughness under the conditions of plane-strain deformation, there were tested the specimens made of steel 34HMA and sizing 12 x 11 x 55 mm. The specimens featuring a notch and a fatigue crack were tested for static load bending. Side notches were made to add to the rigidity of the specimens in the stressed state. The minimum cross section of all the specimens was constant (8 x 10 mm). The specimens were cut out of the central portions of the disks intended for spin testing. Specific fracture energies G_{Ic} obtained during the spin tests of the solid and welded disks were compared with the specific fracture energies determined during static load bending tests of small-size specimens by reference to the stress and crack opening displacement, as it is recommended in the literature (3, 10). Besides, specific fracture work A/F was determined by reference to the area of the diagram of deformation till the maximum load relative to the area of the specimen minimum cross-section. The specimens were tested at temperatures of 80, 20, -40 and -80 °C, in accordance with a special procedure, with the record of the load-deflection diagram. The crack opening displacement was determined by the Ford's formula (11) after which the obtained results were checked by making direct measurements of the crack opening displacement with the use of the microscope.

The data presented in Fig. 8 show that none of the methods used for processing the results of testing specimens for the static bending the results close to the values of G_{Ic} obtained during disk testing. Thus, the increase of the rigidity of the stressed state by increasing the concentration of stresses can not make for the effect of the scale so that it seems impossible to obtain the valid values of the fracture toughness on the small-size specimens.

6. Estimation of structural strength of turbine rotors with use of linear fracture mechanics methods.

Since the nominal inertia load on the rotors of the low-pressure cylinders is obtained during starting, when the rotor temperature is close to the room temperature, all the calculations are based on the assumption that the operating temperature T_o equals +20 °C.

50 % FATT for the welded rotors No. 1 equals 29 °C as determined on the specimens with the Charpy-V notch made in the centre of the full-scale disk (steel 34HMA) since the minimum fracture toughness of this steel is observed in the base metal which was proved by the spin tests of the one piese and welded disks made of this steel. For the rotors Nr. 2 this temperature equals +10 °C.

By the use of the generalized diagram shown in Fig. 6 it becomes possible to determine the minimum values of the stress intensity factors on the lower boundary of the spread band (curve 1) which accordingly equal 214 and 270 $kg/mm^{3/2}$ at the specified values of T_e.

The amounts of stresses for the mostly stressed points of the rotors rotating at a nominal speed or at a speed which exceeds the nominal one by 25 % for the rotor No. 1 and by 20 % for the rotor No. 2 were taken

from the Manufacturer's calculations.

The critical dimensions of the defects were determined by the formulas presented in (12). The critical stresses were determined with the use of the same formulas while the dimensions of the defects were assumed to be equal to the macimum rated values for the welded rotors, i.e. single defects with the equivalent diameter of 4 mm and 6 mm which are sometimes neglected by mutual agreement, and elongated defects with the equivalent diameter of 2 mm. It is known that actual defects may extend through an area which is three times as much as the area of the defects with the equivalent dimensions. Therefore, the calculations were based on the assumption that there may be round defects with the radius of 5 mm (equivalent diameter 6 mm), semi-ellyptical defects with the height of 3,5 mm (equivalent diameter 4 mm) and continous defects with the height of 2 mm (equivalent diameter 2 mm).

The safety factor of the structural elements was determinded as a ratio of the critical stress to the element maximum stress which ist exactly true only when the critical stress does not exceed the yield stress of the material. However the use of this method at higher (non-valid) values of the critical stresses is rather useful since it makes possible comparison of the safety of the structures that are being designed with those that have been already put into service.

The results of the calculations are given in the Table. The safety factor of the mostly stressed points of the welded rotor Nr. 1 is not less than 2,0 and the critical stresses are not less than 72 kg/mm^2 at material yield stress of 50 kg/mm^2. Thus, the brittle fracture of this rotor ist impossible provided that the sizes of the defects do not exceed the tolerances. The safety factor

of the welded rotor No. 2 at higher stresses and at the material of somewhat improved properties is approximately the same as the safety factor of rotor No. 1.

The minimum safety factor of the one piece forged rotor No. 2 is considerably less than that of the welded rotor and equals 1.28 which is due to a higher level of the acting stresses (σ_{max} = 69 and 48.2 kg/mm^2, respectively). The level of the critical stresses of the one piece forged rotor may be increased by increasing the fracture toughness. Thus, to obtain the safety factor of 2.0, the value of K_{Ic} should be equal to 422 kg/mm$^{3/2}$, which in accordance with the generalized diagram of the fracture toughness corresponds to T_e = +36 °C and 50 % FATT = -16 °C. The above data show the advantages of the welded rotors since their safety is ensured by use of the material prossessing lower values of K_{Ic}. It is quite evident that this statement is true at high quality of the welded joint and heat affected zones.

Shown in Fig. 9 are the results of calculations of the increase of the defects in the rotor No. 2 inaccordance with Wilson's formula (9) which takes into account the effect of cyclic starting and stoppings.

The calculations were based on the relationship between the rate of the crack ectension and the stress intensity factor (Fig. 10) obtained by way of experiments on steel 24HN2MFA. The curves presented in Fig. 9 show the size of the initial defects which may increase till their critical values in the course of application of a certain number of the loading cycles. As it is evident from Fig. 9, neither the normal number of the loading cycles associated with the development of the normal power rating (1000 - 2000 cycles for the powerfull turbine) nor the emergency increase of the speed within 20 - 50 cycles will lead to a substantial in-

crease of the dimensions of the dangerous defects. Hence, the cyclic loading of the rotors that have been investigated which is associated with their startings and stoppings does not substantially affect the safety factors calculated during rotor operation.

Conclusions

1. It seems impossible to estimate the tendency of the materials to brittle fracture by reference to the transition temperatures determined by specific values of the impact toughness since this characteristics depends to a great extent on the sharpness of notches and dimensions of the specimens.

2. To make a qualitative comparative estimation of the tendency of the materials to brittle fracture, it is exedient to use the specimens with the Charpy-V notches and to determine the transition temperature by reference to 50 % shear texture (50 % FATT).

3. It has been experimentally proved that the valid values of the stress intensity factor K_{Ic} obtained on the notched disks and on the specimens, types WOL and CT, are practically identical and under definite conditions these values may be used as a basis for the qualitative estimation of the tendency of the materials to brittle fracture, with due regard to the concepts of the linear fracture mechanics.

4. On the basis of the experimental data and data obtained from publications there has been plotted a generalized diagram of the fracture toughness $K_{Ic} = f(T_e)$ which makes it possible to determine the minimum values of K_{Ic} provided that the results of the impact tests of the specimen with notches of the Mesnager or Charpy-V are known.

5. It seems impossible to estimate the level and temperature dependence of the fracture toughness obtained during the spin tests ot the disks and during static bending of small-size prismatic specimens with additional side notches since during these tests the condition of plane-strain deformation is not satisfied.

6. The structural strength certain one piece forged and welded rotors of the turbines has been estimated with due regard to the concepts of the linear fracture mechanics and it has been shown that the reliability of the welded rotors is somewhat higher in case of a high- quality welding.

Bibliography

1. I.V.Navrotskiy, V.I.Baguzin, Zavodskaja laboratorija, 1966, No.7
2. V.P.Rabinovitch et al., Strength problems, 1970, No. 12
3. D.H.Winne, B.M.Wundt, Transactions of the ASTM, Vol. 80, 1958, No.8, p. 1623 - 1658
4. E.T.Wessel, Engineering Fracture Mechanics, Vol. 1, 1958, p. 77 - 103
5. T. Ingham et al., Practical application of fracture mechanics to pressure vessel technology, AIME Publication, London, 1971, p. 200
6. H.D.Greenberg et al., Engineering Fracture Mechanics, Vol. 1, 1970, p. 653 - 674
7. A.I.Brothers et al., Results of bursting tests of alloy steel disks and their application to design against brittle fracture. Paper No. 93, 1965, Presented of the ASTM Annual Meeting, ASTM, Philadelphia
8. M.Orna, Experimental research of rotating disk strength, Schkoda-reviev, 1971, No. 1
9. E.T.Wessel et al., Fracture 1969, Proceeding of the Second International Conference on Fracture, April 1969, p. 825, Chapman and Hall, London, 1969
10. G.R.Irvin et al., In: Technology of steel pressure vessels for water-cooled nuclear reactors. ORNL-NSIC, 21, Dec. 1967
11. C.Ford et al., Journ. Iron and Steel Inst., 1967, Vol. 205, p. 854
12. Fracture Toughness testing and its applications, ASTM STP 381, 1964

Results of calculating rotor safety factors

Shape and location of defect	Type of rotor, value of K_{Io} in kg/mm$^{3/2}$	Effective stress, kg/mm^2		Critical defect size, mm	Permissible defect sizes, mm		Critical stress σ_{cr} kg/mm^2	Safety factor $n = \sigma_{cr}/\sigma_{max}$
		nom	max		equivalent dia. (ultrasonic inspection)	actual size		
Round defect in radial-axial direction, in centre of mostly stressed disk	Welded No.I, 2I4	25.3	39.5	radius 23	6	radius 5	88	2.22
	Welded No.2 270	34.5	48.2	radius 24.5			I08	2.24
Through defect of constant height in radial -axial direction, in centre of mostly stressed disk	Welded No.I 2I4	25.3	39.5	height I8.5	2	height 2	I20	3.04
	Welded No.2 270	34.5	48.2	height 20			I52	3.I5
Angular defect from internal surface in radial-circumferential direction, at joint of middle shell and stiffening disk	Welded No.I 2I4	I8.0	28.0	height I7.5	2	height 2	I00	3.57
	Welded No.2 270	22.I	32.0	height 2I.0			I20	3.75
Semi-elliptical defect extending on to internal surface of cilindrical shell, in radial-axial direction	Welded No.I 2I4	23.0	36.0	height I4 length 46	4	height 3.5 length I2	72 / 92	2.00 / 2.33
	Welded No.2 270	27.4	39.5	height I9 length 63				
Semy-ellyptical defect extending to central drilling, in radial-axial direction	Forged No.2 270	48.0	69.0	height 59.7 length I9	4	height 3.5 length I2	88.5 / I38	I.28 / 2.00
	Forged No.2 422	48.0	69.0	height I45 length 48				

Captions to Figures

Fig. 1. Results of testing specimens made of disk metal welded by manual welding with use of electrode CL-30. Specimens were cut out after spin tests.

Fig. 2. Stress intensity factors K_{Ic} of tested disks versus excessive temperature T_e.

Fig. 3. Variation of fracture toughness and yield stress at decrease of test temperature. Valid values of K_{Ic} are marked with dark symbols.
◑ - CT-3T, ▫ - CT-2T, ▽ -WOL-4X, ● - disks, ▲ - WOL-2X, ◐ - average value of K_{Ic} obtained on specimens WOL-2X with crack of 0.7 W in depth, 1 - steel 24HN2MFA, 2 - steel 18FDOV

Fig. 4. Dependence of rotational factor r on displacement determined by displacement gauge on specimens CT-2T

Fig. 5. Comparison of K_{Ic} values determined by reference to forces and crack opening displacement values on specimens of 50 mm in thickness (steel 18FDOV). o - CT-2T, ◐ - WOL-2X, o, ◐ - K_{Ic} values determined by reference to force values. Valid values of K_{Ic} are marked with dark simbols. ϙ, ϙ - K_{Ic} values determined by reference to crack opening displacement values with due regard to variation of rotational factor, ◌́, ◌́ - K_{Ic} values determined by reference to crack opening displacement values without regard to variation of rotational factor.

Fig. 6. Generalized diagram of $K_{Ic} = f(T_e)$ for perlits steels with yield stresses within 40 - 120 kg/mm^2

Fig. 7. Generalized diagram and impact test results

Fig. 8. Comparison of specific fracture energy determined on disks and on small-size specimens with notches in welded metal applied by electrode CL-30 (a) and wire 08HN2M (b)
o - disks, ● - specimens with side notches,
◐ - specimens with side notches and fatigue crack

Fig. 9. Variation of sizes of defects in welded and one piece rotors versus number of loading cycles.
1 - radius of round defect located in centre of welded rotor disk at $\Delta\sigma = 34.5$ kg/mm^2, K_{Ic} = 270 kg/mm$^{3/2}$;
2 - same as in curve 1 at $\Delta\sigma = 48.5$ kg/mm^2, K_{Ic} = 270 kg/mm$^{3/2}$;
3 - height of semi-elliptical defect extending beyond central drilling of one piece forged rotor, $\Delta\sigma = 69$ kg/mm^2, K_{Ic} = 422 kg/mm$^{3/2}$;
4 - same as in curve 3, $\Delta\sigma = 48$ kg/mm^2, K_{Ic} = 270 kg/mm$^{3/2}$;
5 - same as in curve 3, $\Delta\sigma = 69$ kg/mm^2, K_{Ic} = 270 kg/mm$^{3/2}$

Fig. 10. Rate of crack extension versus variation of K_{Ic} on specimens WOL-4X made of steel 24HN2MFA at normal temperature

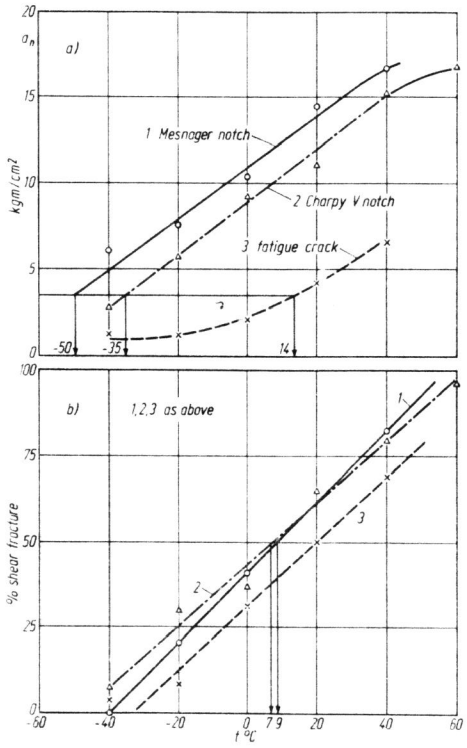

Bild 1.

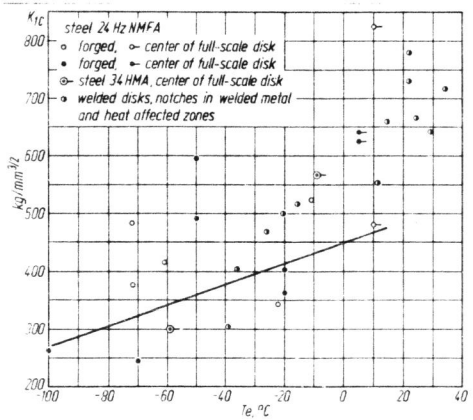

Bild 2.

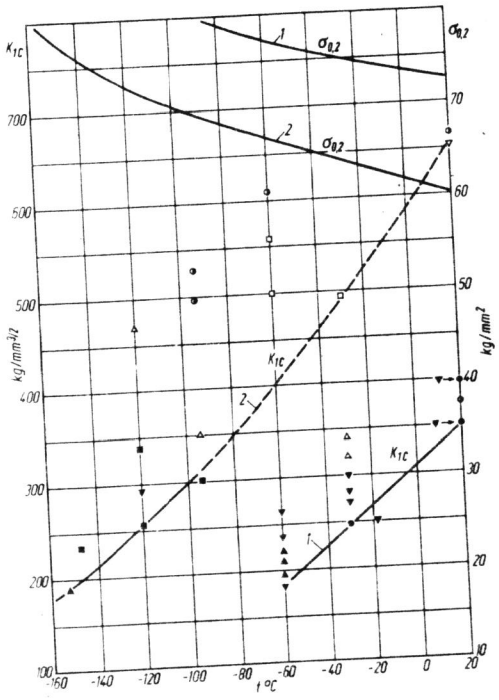

Bild 3.

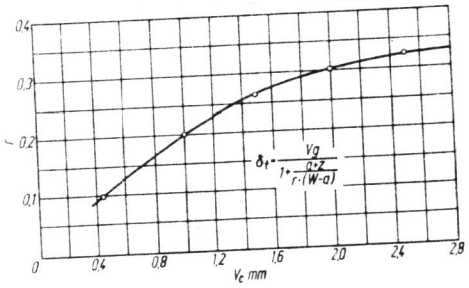

Bild 4.

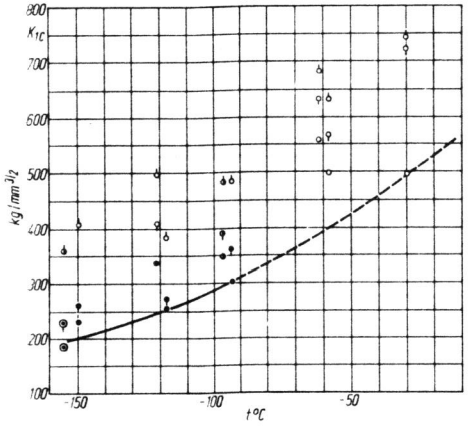

Bild 5.

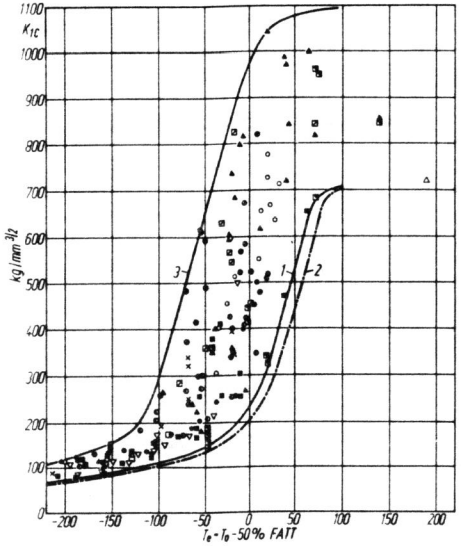

Bild 6.

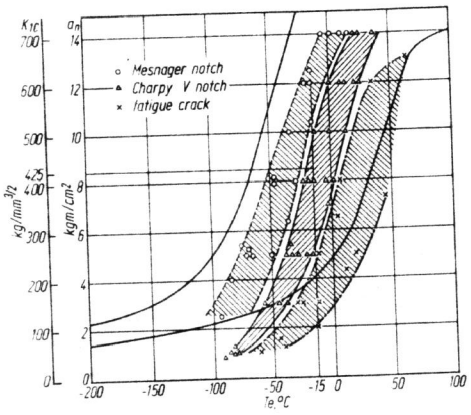

Bild 7.

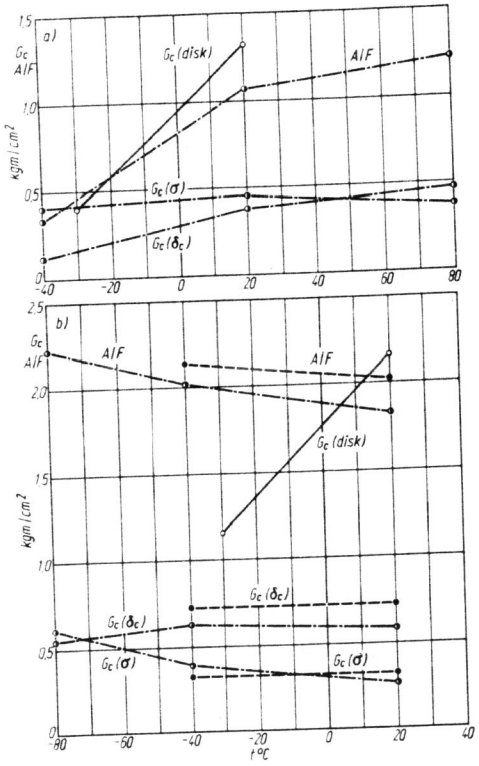

Bild 8.

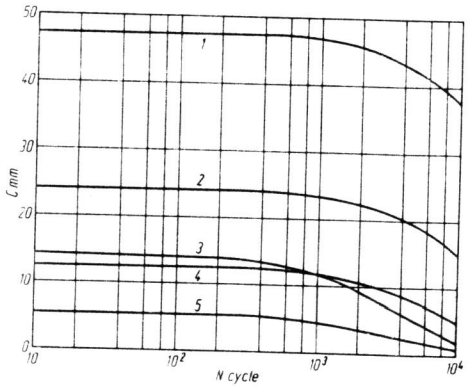

Bild 9.

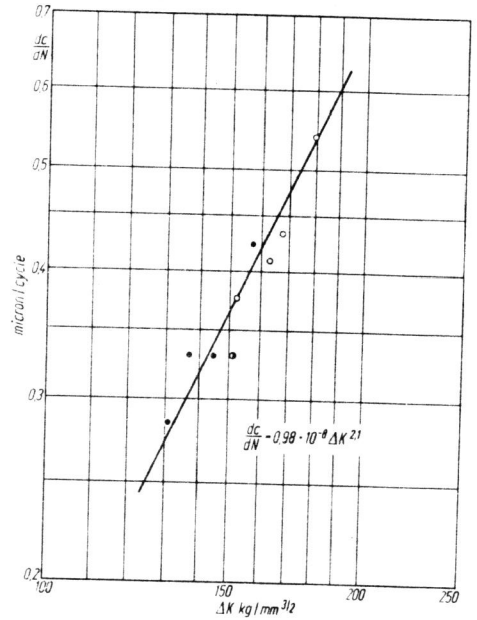

Bild 10.